In vivo fibre optic confocal imaging of microvasculature and nerves in the rat vas deferens and colon

G. D. PAPWORTH,[1] P. M. DELANEY[2], L. J. BUSSAU[1], L. T. VO[1] AND R. G. KING[1]

[1] *Department of Pharmacology, Monash University, Clayton, and* [2] *Optiscan Imaging Ltd., Notting Hill, Victoria, Australia*

(*Accepted 28 January 1998*)

ABSTRACT

A fluorescence confocal microscopy technique was employed to obtain subsurface images of nerve and microvascular structure in the vas deferens and colon of the living rat. The use of dual labelling with vital dyes and 2-channel confocal acquisition allowed differentiation of microscopic structure at both low and higher magnification. Characteristic staining patterns of nerves and blood vessels were repeatedly obtained in each tissue, suggesting the potential of this technique for studying morphological changes associated with surgical procedures and/or models of neuronal or vascular pathology.

Key words: Myenteric plexus; vasculature.

INTRODUCTION

When viewing thick translucent specimens with a conventional light microscope, light returning from out-of-focus elements in the sample severely degrades the quality of the image obtained. Thus fluorescence and reflectance images of samples suffer from reduced contrast (White et al. 1987; Brakenhoff et al. 1989). This is particularly a problem in fluorescence microscopy of biological materials where a fluorescent structure to be imaged may lie above a thick layer of similarly fluorescing material.

The technique of confocal microscopy (as first described by Minsky, 1957) has in recent years become established as a useful research tool in cell biology. Confocal microscopy also appears to be well suited to in vivo microscopic imaging of living tissues, since its optical sectioning capabilities within thick translucent specimens such as biological tissues, enables 3-dimensional reconstruction. Previously we have confocally imaged several tissues in vivo, including microvasculature of rat colon (Delaney et al. 1993), microvasculature of rat gingiva and skin (Papworth et al. 1995), cellular and microvascular structure of hairless mouse skin (Bussau et al. 1995) and rat colonic mucosal structure (Delaney et al. 1994*b*). Several other groups have also begun to explore the possibilities of using confocal microscopy to image a variety of tissues in vivo. These include skin (New et al. 1991; Rajadhyaksha et al. 1995), teeth (New et al. 1991; Watson et al. 1992), eye (Petroll et al. 1993; Auran et al. 1994; Beuerman et al. 1994; Chew et al. 1995; Wiegand et al. 1995; Jester et al. 1995, 1996), brain vasculature (Villringer et al. 1990, 1991; Lorenzl et al. 1993; Lindauer et al. 1996), kidney (Andrews et al. 1991; Pulver et al. 1993; Andrews, 1994), and epididymis, adrenal glands, liver, thyroid, muscle, nerve and connective tissue (Jester et al. 1991). However, the bulky nature of conventional confocal microscopes, combined with movement artifacts (e.g. due to respiration) has hindered the progress of in vivo confocal microscopy. The fibre optic confocal imaging microscope (as described by Delaney et al. 1994*a*) replaces a pinhole (used to deliver and/or collect light in the conventional confocal microscope) with an optical fibre, giving a reduction in bulk optics at the imaging end, and therefore a more mobile instrument suited to in vivo work. In this report we describe the in vivo fibre optic confocal imaging of components of the enteric nervous system and microvasculature in the rat colon, and imaging of nerves and vessels in the rat vas deferens. The development of vital staining techniques necessary to allow this imaging is also discussed.

Correspondence to Dr Glenn D. Papworth, Department of Pharmacology, Monash University, Clayton, Victoria 3168, Australia. Tel: +61 3 9905 5397; fax: +61 3 9905 5851.

METHODS

The fluorescent dye 4-(4-(diethylamino)styryl)-*N*-methylpyridinium iodide (4-di-2-ASP) was used topically to image the intact descending colon of the rat (imaged from the serosal surface) and also nerves associated with the vas deferens microvascular bed in vivo. In certain experiments the fluorescent tracer molecule fluorescein isothiocyanate-conjugated dextran (FITC-dextran, MW 150 kDa) was administered intravascularly in combination with topically applied 4-di-2-ASP.

Animals

All experiments were approved by the institutional committee for ethics in animal experimentation and conformed to the Australian National Health and Medical Research Council Guidelines. Male Sprague-Dawley rats (200–300 g) were used. For all in vivo rat experiments, animals were anaesthetised with urethane (0.25 g/100 g body weight i.p.). Depth of anaesthesia was monitored continuously throughout the duration of the experiments by a rear paw pinch test, and booster doses of anaesthetic were administered i.p. to maintain surgical anaesthesia when required. A jugular vein cannula was inserted if required for intravascular dye administration.

Dyes

The concentration of the dyes applied and the period of staining (for 4-di-2-ASP) in both preparations was determined following extensive trials of different staining conditions with visual evaluation of image quality for each condition. For the dual channel experiments, the fluorescent intensity of the staining needed to be matched between the dyes in vivo so that the effective fluorescence of the 4-di-2-ASP-stained nerve fibres was of similar brightness compared to the fluorescence of the vessels labelled following FITC-dextran administration.

4-di-2-ASP. 4-di-2-ASP is a vital stain specific for nervous tissue which may be used for confocal microscopy without processing of the tissue. In both the vas deferens and colon preparations, 4-di-2-ASP was topically applied (10 μM, 3 min staining, 1 min saline wash) to the tissue surface following stabilisation.

FITC-dextran. FITC-dextran (MW 150 kDa, Sigma, USA) is a commonly used intravascular dye. FITC-dextran was administered via a cannulated jugular vein (0.5 ml, 10 mg/ml in saline) when required.

Organ exposure

Vas deferens. A midline abdominal incision was made in the anaesthetised rat, and the intact vas deferens was exposed and stabilised by positioning it across gauze, keeping it continually soaked with warmed saline. An adjustable micrometer with a 20 mm diameter metal micropositioner ring was used for stabilisation of the surrounding tissue, without applying any pressure directly to the vas deferens itself. The animal was then transferred to a specialised heated platform attached to the confocal microscope stage, enabling maintenance of body temperature at 37 °C (monitored by a rectal thermometer). The number of experiments were as follows: single channel ($n = 8$), 2 channel ($n = 12$).

Colon. Following anaesthesia, a 10 mm region of the descending colon was exposed and stabilised as described above for the vas deferens, and 4-di-2-ASP was topically applied. The number of experiments were as follows: single channel ($n = 15$), 2 channel ($n = 8$).

Confocal microscopy

Both single and multichannel fluorescence confocal imaging was performed using the Optiscan F900e fibre optic laser scanning confocal microscope system equipped with an argon ion laser. Single channel fluorescence imaging was performed using an excitation wavelength of 488 nm (blue), with detection > 514 nm (green). Two channel fluorescence imaging was performed with channel 1 excitation at 488 nm (blue), detection using a 515–550 nm band-pass filter (green), and channel 2 excitation at 488 nm (blue), detection using a 590 nm long-pass filter (red). The confocal system was fitted to an Olympus BH-2 light microscope equipped with Olympus objectives ($\times 10$, 0.4 NA, calculated optical slice thickness = 7 μm, or $\times 20$, 0.7 NA, calculated optical slice thickness = 2 μm). All images presented were single scan images representing one focal plane within the tissue. Gain and aperture settings were held constant within individual experiments. All images shown are raw image data that has not undergone any form of image processing.

In the vas deferens, imaging was performed through the intact external surface. Similarly, in the colon, imaging was performed through the intact serosal surface. At the end of each experiment, the animal was killed by anaesthetic overdose.

RESULTS

For all presented figures, higher magnification images are from fields wholly independent from the corresponding low-power images.

Vas deferens: single channel imaging

Topical staining of the exposed rat vas deferens in vivo with 4-di-2-ASP according to the protocol described above enabled consistent imaging of nerve fibres and blood vessel walls. Figure 1*a* shows 4-di-2-ASP brightly staining the walls of a component of the microvasculature, with associated nerve fibre tracts also visible. Higher magnification imaging (Fig. 1*b*) showed that this technique can allow visualisation of nerve elements such as ganglia (which are quite scattered in this tissue) and secondary fibre bundles.

Colon: single channel imaging

Various nerve components were identifiable in in vivo subsurface confocal images of the rat myenteric plexus. Visible in Figure 2*a* are ganglia, primary fibre

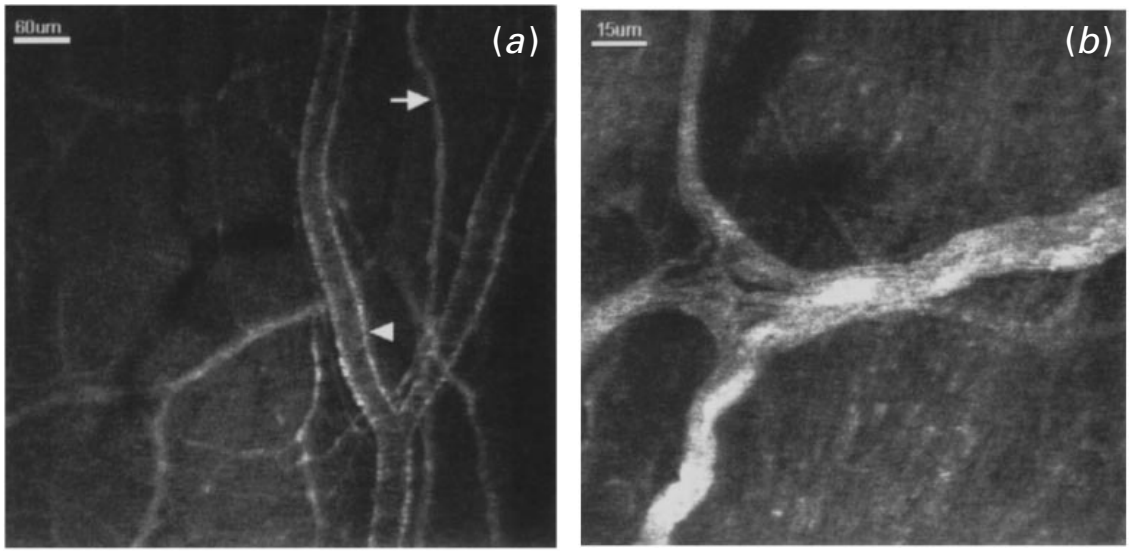

Fig. 1. Single channel confocal microscopy of rat vas deferens in vivo following topical application of 4-di-2-ASP. (*a*) Low magnification view of fine nerve fibres (arrow) and blood vessel walls (arrowhead). At higher magnification (*b*) a nerve ganglion can be seen with secondary fibre bundles. Calculated optical slice thicknesses: *a*, 7 μm; *b*, 2 μm.

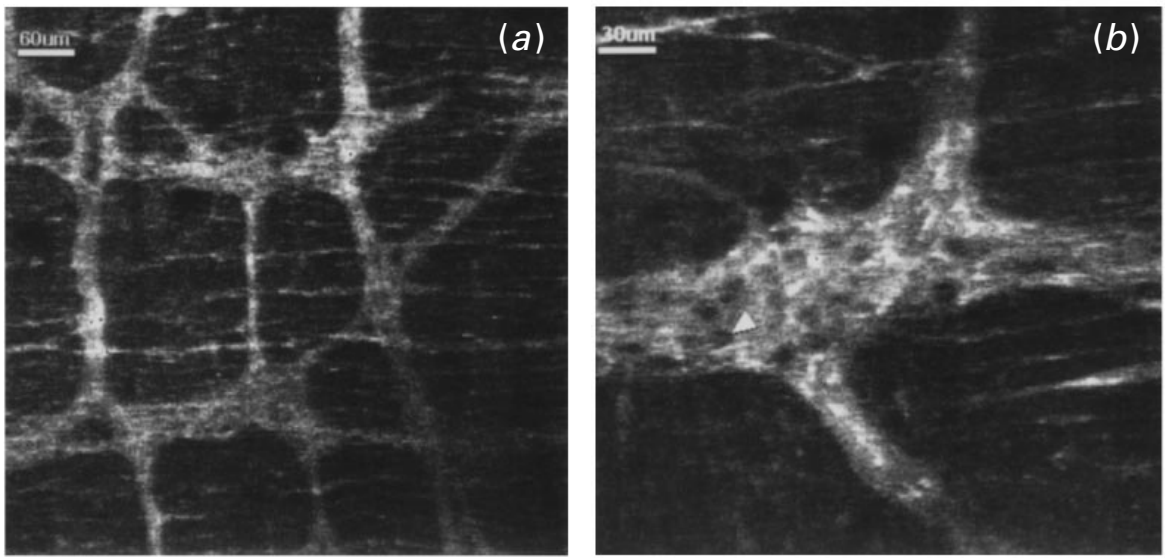

Fig. 2. Single channel confocal microscopy of rat colon in vivo following topical application of 4-di-2-ASP. (*a*) Myenteric plexus showing ganglia, primary fibre tracts, and secondary fibre bundles. (*b*) Ganglion containing neuronal cell bodies (dark shapes, arrowhead); fine nerve fibres that are part of the tertiary nerve plexus are also visible. Calculated optical slice thicknesses: *a*, 7 μm; *b*, 2 μm.

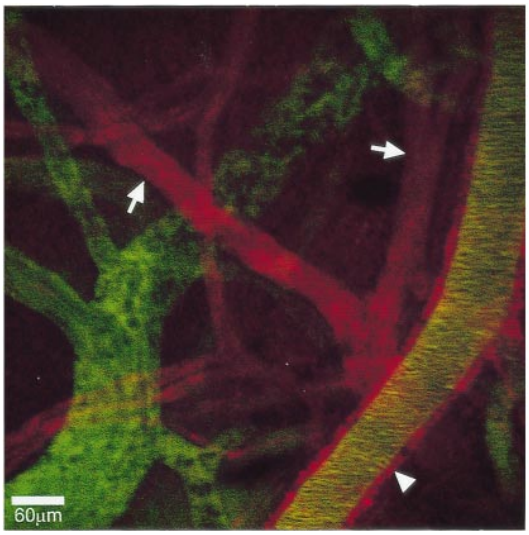

Fig. 3. Dual channel confocal microscopy of rat vas deferens following topical 4-di-2-ASP and i.v. FITC-dextran. In the lower left, blood cells can be seen as dark shapes against the green of a blood vessel and its branches. Large branching nerve fibres are visible in red (arrows). Also visible is another large blood vessel, with distinctive red staining of the wall region of the vessel by 4-di-2-ASP (arrowhead). Calculated optical slice thickness: 7 μm.

tracts, and secondary fibre bundles. At higher magnification (Fig. 2*b*) an individual ganglion and fibre tracts are seen, along with finer nerve fibres that are part of the tertiary nerve plexus. Within the ganglion, neuronal cell bodies are outlined as dark shapes.

Vas deferens: simultaneous dual channel imaging

Figure 3 shows typical results obtained with the dual channel in vivo technique for imaging the rat vas deferens, and illustrates how it enabled good differentiation between the subsurface microvasculature and associated nerve structure. Green represents detection of the emission wavelength of the vascular plasma stain FITC-dextran, which indicates the blood vessel lumen. Red represents detection of the emission wavelength of 4-di-2-ASP, which stains nerves. During all experiments, blood cells could be seen moving within vessels. In Figure 3 blood cells (dark shapes against the green plasma stain) can be seen in one blood vessel and its several branches. Large nerve fibres are also visualised in this figure, staining distinctly red and branching throughout the image. Also visible is another large blood vessel, with its lumen stained green by FITC-dextran, but which also has distinctive red staining of the wall of the vessel by 4-di-2-ASP, indicating possible staining of nerve components of the vascular wall.

Figure 4*a* and *b* show single slice images of the same 2 adjacent blood vessels, one of which shows staining with 4-di-2-ASP (red). The image in 4*b* was acquired approximately 20 μm above the plane of 4*a*. Visible quite clearly in 4*b* is red staining due to 4-di-2-ASP extending over the upper surface of one of the blood vessels. In Figure 4*a*, however, only the lateral 'edges' of the same vessel are visible as red stained due to this single slice being taken through the middle of the vessel lumen, thus not showing the 'upper' vessel wall. Thus 4-di-2-ASP appears to be staining components of the perivascular nerve plexus (red) of this blood vessel. Note that the adjacent vessel showing only the green staining of the lumen remains effectively

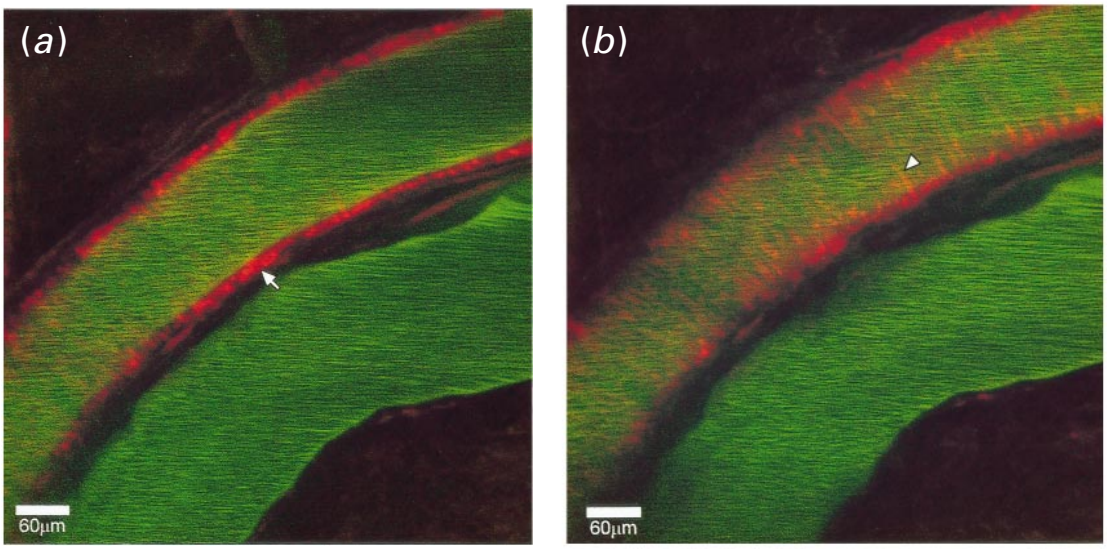

Fig. 4. Dual channel confocal microscopy of rat vas deferens following topical 4-di-2-ASP and i.v. FITC-dextran. (*a*) Single slice image of 2 adjacent blood vessels, one of which shows staining with 4-di-2-ASP on the lateral 'edges' of the vessel (red, arrow). (*b*) The same vessels but at a level approximately 20 μm above the plane of *a*. Visible quite clearly in *b* is red staining extending over the upper surface of the blood vessel (arrowhead). Calculated optical slice thicknesses: *a*, 7 μm; *b*, 7 μm.

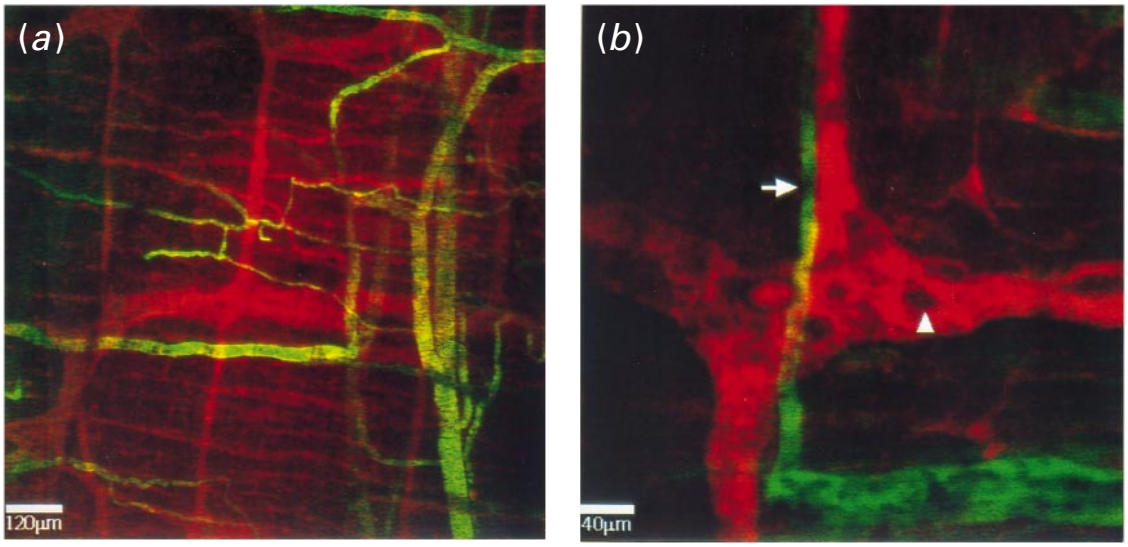

Fig. 5. Dual channel confocal microscopy of rat colon following topical 4-di-2-ASP and i.v. FITC-dextran. (*a*) Components of the myenteric plexus (red) and associated blood vessels of various sizes (green). Cell bodies (arrowhead) are visible within a ganglion at higher magnification in *b*. Also shown is an overlying blood vessel in which a single blood cell column is visible (arrow). Fine nerve fibres can be seen outside the ganglion. Calculated optical slice thicknesses: *a*, 7 μm; *b*, 2 μm.

unchanged in appearance between panels *a* and *b* of Figure 4.

Colon: simultaneous dual channel imaging

Dual channel imaging enabled identification of the same nerve components of the myenteric plexus as were visible with single channel imaging, as well as showing the spatial relationship of the myenteric plexus with components of the microvasculature. Figure 5*a* shows the essentially planar nature of the myenteric plexus with few visible blood vessels running through this plane. At higher magnification (Fig. 5*b*), a myenteric plexus ganglion containing nerve cell bodies as dark shapes can be seen, but also visible are overlying vascular components with blood cells visible as dark shapes. Fine nerve fibres can also be seen in the background of the image. Unlike in the vas deferens, this dual labelling technique did not show any microvascular components with 4-di-2-ASP-stained vessel walls.

DISCUSSION

To be useful in experimental and clinical studies for in vivo imaging of the enteric nervous system and other autonomic nerves, a fluorescent vital dye must be nontoxic and without pharmacological effects on the tissue; preferably water soluble; nonfading; visible without further manipulation of the tissue; and specific for nervous tissue (Hanani, 1992). 4-di-2-ASP has been shown in prior work to fulfil all these requirements. 4-di-2-ASP is classified as a fast response styryl dye. Although its mechanism of staining action is not completely clear, it is thought to stain nerves preferentially (Molecular Probes Inc., personal communication, 1995).

Hanani et al. (1993) suggested that a rapid and reliable technique that does not require sectioning would be useful for examining the enteric nervous system for evidence of certain pathologies of the gut. Many of the existing methods used for vitally staining the intact enteric nervous system have proved unsuitable because they involve fixation or are time consuming or expensive procedures (Hanani, 1992), e.g. staining for acetylcholine esterase or silver impregnation. Immunohistochemical staining of nerve elements is sensitive and selective, but is also slow and expensive. Hanani reported the successful use of the vital fluorescent dye 4-di-2-ASP for examining unfixed whole mount bowel specimens from patients with Hirschsprung's disease (characterised by aganglionosis of the diseased segment of gut), using epifluorescent illumination. This method however required a biopsy to be taken, the tissue pinned out and the mucosa, submucosa and circular muscle removed under a dissecting microscope to expose the myenteric plexus for visualisation under a conventional epifluorescence light microscope. This was necessary due to the depth of the plexus within the gut wall, since the myenteric plexus lies between the outer longitudinal and inner circular muscle layers of the muscularis externa. Miura et al. (1996) also discussed the difficulties inherent in the use of stereo or electron microscopes to

observe plexus structure following stripping off of muscle layers of whole mount samples. Other workers have used topically applied fluorescent dyes and confocal microscopy of in vitro mounts of gut mucosa to study various aspects of colonic crypt function, including fluid absorption (Naftalin et al. 1995) and quantitation of cell cycle biomarkers (Konishi et al. 1996). Fiarman et al. (1995) used confocal microscopy to examine regional differences in autofluorescence in human colonic mucosa samples.

Confocal microscopy of the colon has rarely been performed in living animals, with the exceptions of a study on mouse colonic mucosa where confocal microscopy was used as a tool for measuring parameters of colonic crypt function (Chu et al. 1995) and a study of rat colonic mucosal structure (Delaney et al. 1994*b*).

The results presented here show the successful use of confocal microscopy to visualise subsurface morphology of nerves and blood vessels in the rat colon in vivo. Because these images were taken from the serosal side of the intact colon, the imaging was therefore performed through the layer of serosa and the intact longitudinal muscle layer. This illustrates well the 3-dimensional 'optical sectioning' capabilities of the confocal microscope which give this technique potential for imaging the architecture of the myenteric plexus in normal or diseased segments of gut.

Herrera & Banner (1990) performed one of the few in vivo studies involving 4-di-2-ASP, and imaged stained nerve terminals at neuromuscular junctions using a conventional fluorescence microscope. In their study, as well as staining unmyelinated regions of motor axons, 4-di-2-ASP also stained components of the microvasculature and fine unmyelinated axons, probably autonomic or sensory, associated with this microvasculature. Capillaries did not stain, but the walls of larger vessels stained brightly, suggesting that 4-di-2-ASP was staining nerves in the vessel walls. Our confocal imaging following staining with 4-di-2-ASP suggests that this dye has similar staining properties in vas deferens in vivo. The dual labelling experiments with separate channel detection of the emission wavelengths of each fluorophore gave clear identifiable separation between vascular and nerve structure, with the walls of some blood vessels appearing brightly stained with 4-di-2-ASP. To our knowledge, no other workers have imaged subsurface nerve and microvascular structure in the living rat vas deferens in this manner. These images suggest the possible use of this technique in studying changes in neuronal and/or vascular morphology arising from surgical procedures, for example denervation following vasectomy (DeGaris & Pennefather, 1986) or reinnervation following vasovasostomy (DeGaris & Pennefather, 1987).

Thus in this report we have described the establishment of an imaging technique useful as a means of observing and morphologically characterising living neuronal and vascular elements simultaneously in vivo. Further investigation may show this technique to be useful as a tool in the study of neurodegenerative disorders and/or vascular pathology in animal models, and potentially in humans.

REFERENCES

Andrews PM (1994) The histopathology of kidney uriniferous tubules as revealed by noninvasive confocal vital microscopy. *Scanning* **16**, 174–181.

Andrews PM, Petroll WM, Cavanagh HD, Jester JV (1991) Tandem scanning confocal microscopy (TSCM) of normal and ischemic living kidneys. *American Journal of Anatomy* **191**, 95–102.

Auran JD, Koester CJ, Rapaport R, Florakis GJ (1994) Wide field scanning slit in vivo confocal microscopy of flattening-induced corneal bands and ridges. *Scanning* **16**, 182–186.

Beuerman RW, Laird JA, Kaufman SC, Kaufman HE (1994) Quantification of real-time confocal images of the human cornea. *Journal of Neuroscience Methods* **54**, 197–203.

Brakenhoff GJ, van der Voort HTM, van Spronsen EA, Nanninga N (1989) Three-dimensional imaging in fluorescence by confocal scanning microscopy. *Journal of Microscopy* **153**, 155–159.

Bussau LJ, Delaney PM, Papworth GD, Barkla DH, King RG (1995) Fibre optic confocal imaging of hairless mouse skin: comparison with conventional histology. *Proceedings of the Australian Physiological and Pharmacological Society* **26**, 233P.

Chew SJ, Beuerman RW, Kaufman HE, McDonald MB (1995) In vivo confocal microscopy of corneal wound healing after excimer laser photorefractive keratectomy. *CLAO Journal* **21**, 273–280.

Chu, S, Brownell WE, Montrose MH (1995) Quantitative confocal imaging along the crypt-to-surface axis of colonic crypts. *American Journal of Physiology* **269**, C1557–1564.

Corbett MC, Prydal, JI, Verma S, Oliver KM, Pande M, Marshall J (1996) An in vivo investigation of the structures responsible for corneal haze after photorefractive keratectomy and their effect on visual function. *Ophthalmology* **103**, 1366–1380.

Degaris RM, Pennefather JN (1986) Sympathetic denervation of the rat vas deferens following unilateral vasectomy. *Clinical and Experimental Pharmacology and Physiology* **13**, 399–406.

Degaris RM, Pennefather JN (1987) Noradrenergic reinnervation of the rat vas deferens after vasovasostomy following vasectomy. *Clinical and Experimental Pharmacology and Physiology* **14**, 353–360.

Delaney PM, Harris MR, King RG (1993) Novel microscopy using fibre optic confocal imaging and its suitability for subsurface blood vessel imaging in vivo. *Clinical and Experimental Pharmacology and Physiology* **20**, 197–198.

Delaney PM, Harris MR, King RG (1994*a*) Fibre optic laser scanning confocal microscope suitable for fluorescence imaging. *Applied Optics* **33**, 573–577.

Delaney PM, King RG, Lambert JR, Harris MR (1994*b*) Fibre optic confocal imaging (FOCI) for subsurface microscopy of the colon in vivo. *Journal of Anatomy* **184**, 157–160.

Fiarman GS, Nathanson MH, West AB, Deckelbaum LI, Kelly L, Kapadia CR (1995) Differences in laser-induced autofluorescence between adenomatous and hyperplastic polyps and

normal colonic mucosa by confocal microscopy. *Digestive Diseases and Sciences* **40**, 1261–1268.

Hanani M (1992) Visualization of enteric and gallbladder ganglia with a vital fluorescent dye. *Journal of the Autonomic Nervous System* **38**, 77–84.

Hanani M, Udassin R, Ariel I, Freund H (1993) A simple and rapid method for staining the enteric ganglia: application for Hirschsprung's disease. *Journal of Pediatric Surgery* **28**, 939–941.

Herrera AA, Banner LR (1990) The use and effects of vital fluorescent dyes: observation of motor nerve terminals and satellite cells in lining frog muscles. *Journal of Neurocytology* **19**, 67–83.

Jester JV, Andrews PM, Petroll WM, Lemp MA, Cavanagh HD (1991) In vivo, real-time confocal imaging. *Journal of Electron Microscopy Technique* **18**, 50–60.

Jester JV, Petroll WM, Barry PA, Cavanagh HD (1995) Expression of alpha-smooth muscle (alpha-sm) actin during stromal wound healing. *Investigative Ophthalmology and Visual Science* **35**, 809–819.

Jester JV, Maurer JK, Petroll WM, Wilkie DA, Parker RD, Cavanagh HD (1996) Application of in vivo confocal microscopy to the understanding of surfactant-induced ocular irritation. *Toxicologic Pathology* **24**, 412–428.

Konishi H, Steinbach G, Hittelman WN, Fujita K, Lee JJ, Glober GA (1996) Cell kinetic analysis of intact rat colonic crypts by confocal microscopy and immunofluorescence. *Gastroenterology* **111**, 1493–1500.

Lindauer U, Dreier J, Angstwurm K, Rubin I, Villringer A, Einhaupl KM et al. (1996) Role of nitric oxide synthase inhibition in leukocyte-endothelium interaction in the rat pial microvasculature. *Journal of Cerebral Blood Flow and Metabolism* **16**, 1143–52.

Lorenzl S, Koedel U, Dirnagl U, Ruckdeschel G, Pfister HW (1993) Imaging of leukocyte-endothelium interaction using in vivo confocal laser scanning microscopy during the early phase of experimental pneumococcal meningitis. *Journal of Infectious Diseases* **168**, 927–933.

Minsky M (1957) U.S. Patent No. 3,013,467.

Miura H, Ohi R, Tseng SW, Takahashi T (1996) The structure of the transitional and aganglionic zones of Auerbach's plexus in patients with Hirschsprung's disease: a computer-assisted three-dimensional reconstruction study. *Journal of Pediatric Surgery*, **31**, 420–426.

New KC, Petroll WM, Boyde A, Martin L, Corcuff P, Leveque JL et al. (1991) In vivo imaging of human teeth and skin using real-time confocal microscopy. *Scanning* **13**, 369–372.

Naftalin RJ, Zammit PS, Pedley KC (1995) Concentration polarization of fluorescent dyes in rat descending colonic crypts: evidence of crypt fluid absorption. *Journal of Physiology* **487**, 479–495.

Papworth GD, Delaney PM, Bussau LJ, King RG (1995) In vivo subsurface microvascular imaging fibre optic confocal microscopy (FOCI). *Proceedings of the Australian Physiological and Pharmacological Society* **26**, 200P.

Petroll WM, Cavanagh HD, Jester JV (1993) Three-dimensional imaging of corneal cells using in vivo confocal microscopy. *Journal of Microscopy* **170**, 213–219.

Pulver M, Petroll WM, Andrews PM (1993) Noninvasive microscopic evaluation of the intact living nephrotic kidney. *Laboratory Investigation* **68**, 592–596.

Rajadhyaksha M, Grossman M, Esterowitz D, Webb RH, Anderson RR (1995) In vivo confocal scanning laser microscopy of human skin: melanin provides strong contrast. *Journal of Investigative Dermatology* **104**, 946–952.

Villringer A, Haberl RL, Dirnagl U, Anneser F, Verst M, Einhaupl KM (1989) Confocal laser microscopy to study microcirculation on the rat brain surface in vivo. *Brain Research* **304**, 159–160.

Villringer A, Dirnagl U, Them A, Schurer L, Krombach F, Einhaupl KM (1991) Imaging of leukocytes within the rat brain cortex in vivo. *Microvascular Research* **42**, 305–315.

Watson TF, Petroll WM, Cavanagh HD, Jester JV (1992) In vivo confocal microscopy in dental research: an initial appraisal. *Journal of Dentistry* **20**, 352–358.

White JG, Amos WB, Fordham M (1987) An evaluation of confocal versus conventional imaging of biological structures by fluorescence light microscopy. *Journal of Cell Biology* **105**, 41–48.

Wiegand W, Thaer AA, Kroll P, Geyer OC, Garcia AJ (1995) Optical sectioning of the cornea with a new confocal in vivo slit-scanning videomicroscope. *Ophthalmology* **102**, 568–575.